



Contents lists available at ScienceDirect

Earth and Planetary Science Letters

www.elsevier.com/locate/epsl



Does subduction-induced mantle flow drive backarc extension?

Zhihao Chen^{*}, Wouter P. Schellart, Vincent Strak, João C. Duarte¹

School of Earth, Atmosphere and Environment, Monash University, Melbourne, VIC 3800, Australia

ARTICLE INFO

Article history:

Received 10 September 2015
 Received in revised form 5 February 2016
 Accepted 12 February 2016
 Available online xxxx
 Editor: J. Brodholt

Keywords:

subduction
 geodynamic analogue modelling
 subduction-induced mantle flow
 backarc extension
 velocity gradient
 shear traction

ABSTRACT

Backarc extension is a characteristic feature of many narrow subduction zones. Seismological and geochemical studies imply the occurrence of mantle flow around the narrow subducting slabs. Previous 3D models suggested that backarc extension is related to subduction-induced toroidal mantle flow. The physical viability of this mechanism, however, has never been tested using laboratory-based geodynamic models. In this work, we present dynamic laboratory models of progressive subduction in three-dimensional (3D) space that were carried out to test this mechanism. To achieve this, we have used a stereoscopic Particle Image Velocimetry (sPIV) technique to map simultaneously overriding plate deformation and 3D subduction-induced mantle flow underneath and around an overriding plate. The results show that the strain field of the overriding plate is characterized by the localization of an area of maximum extension within its interior (at 300–500 km from the trench). The position of maximum extension closely coincides (within ~ 2 cm, scaling to 100 km) with that of the maximum trench-normal horizontal mantle velocity and velocity gradient measured at a scaled depth of 15–25 km below the base of the overriding plate, and the maximum horizontal gradient of the vertical mantle velocity gradient. We propound that in narrow subduction zones backarc extension in the overriding plate is mainly a consequence of the trench-normal horizontal gradients of basal drag force at the base of the overriding plate. Such shear force gradients result from a horizontal gradient in velocity in the mantle below the base of the lithosphere induced by slab rollback. Calculations based on our models indicate a tensional horizontal trench-normal deviatoric stress in the backarc region scaling to ~ 28.8 MPa, while the overriding plate trench-normal stress resulting from the horizontal component of the trench suction force is about an order of magnitude smaller, scaling to ~ 2.4 – 3.6 MPa.

© 2016 Elsevier B.V. All rights reserved.

1. Introduction

During progressive subduction overriding plates may follow the trench and/or deform internally. Such deformation can involve extension or shortening, or the overriding plate may remain undeformed (neutral). Overriding plate deformation is often characterized by backarc extension, which gives rise to backarc basins (Jarrard, 1986; Dvorkin et al., 1993; Heuret and Lallemand, 2005; Schellart, 2008b). For instance, the Aegean and Tyrrhenian Seas are the backarc basins of the Hellenic and Calabria subduction zones, respectively. Structural geological and geophysical investigations have shown that these backarc basins have experienced extension during the Cenozoic (Angelier et al., 1982; Lister et al., 1984; Lonergan and White, 1997; Nicolosi et al., 2006), while seismological and geodetic investigations indicate that they are actively

extending today (Amato and Montone, 1997; Kahle et al., 2000; D'Agostino and Selvaggi, 2004; Hollenstein et al., 2008).

Plates and the sub-lithospheric mantle are part of one convective system (Elsasser, 1971; Bercovici, 2003). More than forty years ago it was already suggested that subducted slabs are the dominant driving force of this convective system (Elsasser, 1971). Elsasser (1971), and later Shemenda (1993), further proposed that backarc basins directly result from this subduction process due to trench suction (the force perpendicular to the subduction zone interface) induced by slab rollback. Some authors, however, have argued that backarc basins form due to overriding plate collapse resulting from an excess in potential energy (Hatzfeld et al., 1997; Gautier et al., 1999), while other authors suggested that there is a correspondence between backarc extension and subduction-induced mantle flow below the overriding plate, either in a poloidal fashion (Sleep and Toksöz, 1971) or toroidal fashion (Schellart and Moresi, 2013; Meyer and Schellart, 2013; Duarte et al., 2013; Sternai et al., 2014). Despite the abundant attempts to explain the origin of backarc extension, the fundamental driving mechanism is still a matter of debate.

^{*} Corresponding author. Tel.: +61 03 99024207.

E-mail address: zhihao.chen@monash.edu (Z. Chen).

¹ Now at Instituto Dom Luiz and Geology Department, University of Lisbon, Campo Grande, Lisbon, Portugal.

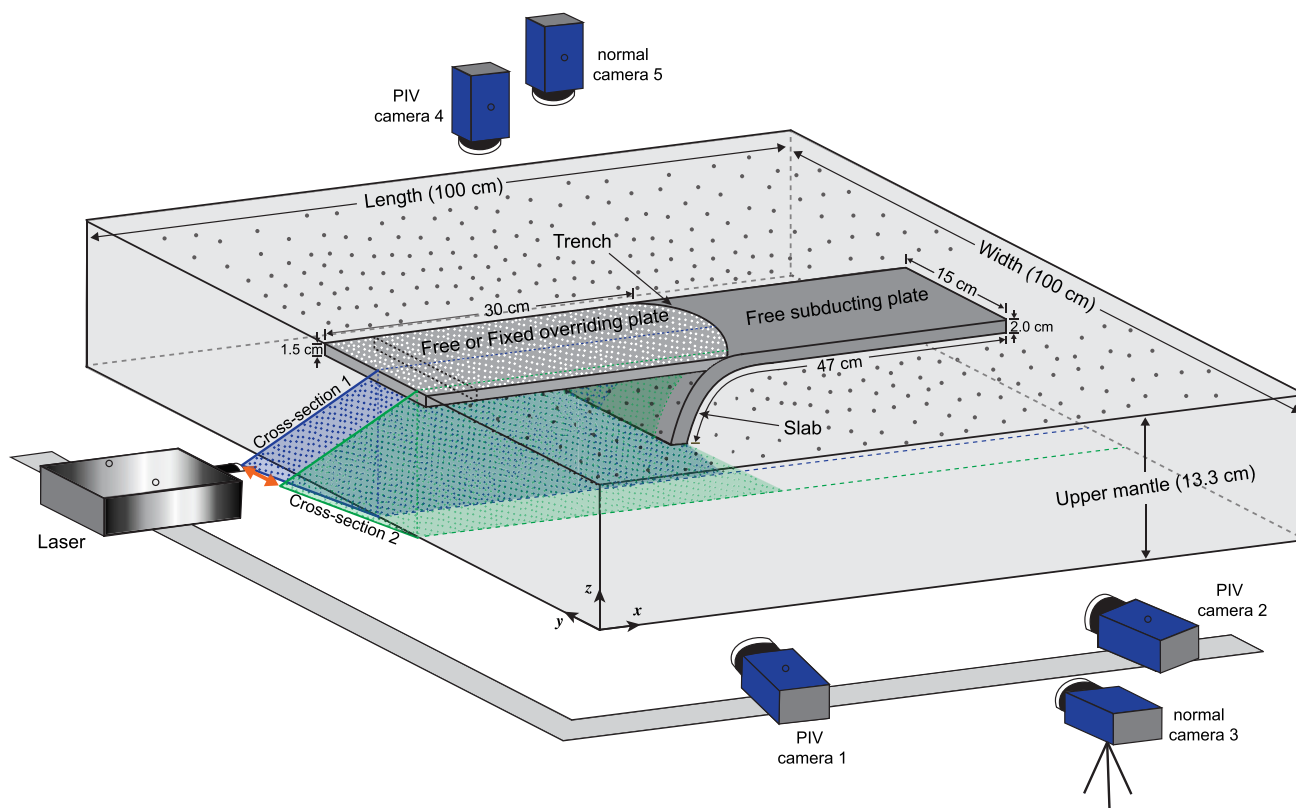


Fig. 1. 3D configuration of the model setup. This setup of subduction includes a free high-viscosity subducting plate, a free/fixed high-viscosity overriding plate, a low-viscosity sub-lithospheric upper mantle and a weak interplate mechanical coupling. The PIV system consists of a laser and three PIV high-resolution cameras. One PIV camera was located above the tank to map the progressive deformation of the overriding plate and mantle flow at the surface, and two PIV cameras were located to the side to map the progressive mantle flow simultaneously in stereo. Two normal cameras (one above and another to the side) were used to record the subduction process. The blue and green dashed lines on the overriding plate indicate the locations of cross-section 1 and cross-section 2, respectively. (For interpretation of the references to color in this figure legend, the reader is referred to the web version of this article.)

Results from seismological and geochemical investigations imply the existence of a 3D subduction-induced mantle flow around lateral slab edges from the subslab zone towards the mantle wedge (Civello and Margheriti, 2004; Zandt and Humphreys, 2008; Hoernle et al., 2008; Long and Silver, 2008; Diaz et al., 2010). Such flow has also been observed in laboratory experiments (Buttles and Olson, 1998; Kincaid and Griffiths, 2003; Schellart, 2004; Funicello et al., 2004; Schellart, 2008a; Druken et al., 2011; Strak and Schellart, 2014; MacDougall et al., 2014) and numerical models of subduction (Piomallo et al., 2006; Stegman et al., 2006; Schellart et al., 2007; Jadamec and Billen, 2010; Li and Ribe, 2012; Faccenda and Capitanio, 2012; Schellart and Moresi, 2013; Li et al., 2014). It has been previously proposed that this subduction-induced mantle flow is responsible for backarc extension (Schellart and Moresi, 2013; Duarte et al., 2013; Sternai et al., 2014). In particular, using geodynamic numerical models of subduction, Schellart and Moresi (2013) presented quantitative results demonstrating that backarc extension at narrow subduction zones is driven by rollback-induced toroidal mantle flow. However, this driving mechanism has not been examined using physical laboratory models of subduction.

In this work we present analogue experiments that for the first time build a direct link between overriding plate deformation and slab rollback-induced mantle flow. We present buoyancy-driven geodynamic models of progressive subduction in 3D space, including a subducting plate, overriding plate, upper mantle reservoir and weak interplate material. A stereoscopic Particle Image Velocimetry (sPIV) technique has been used to simultaneously map the overriding plate deformation and subduction-induced mantle flow below and around the overriding plate. Such a setup allows

us to quantitatively examine the correlation between the overriding plate deformation and the subduction-induced mantle flow.

2. Methods

Our models consist of two layers, following the setups of Duarte et al. (2013) and Meyer and Schellart (2013) (Fig. 1). The top layer is made of a linear-viscous high-viscosity silicone mixed with fine iron powder, simulating a subducting plate (negatively buoyant with density $\rho = 1528 \text{ kg/m}^3$ and dynamic shear viscosity $\eta_{SP} = 6.07 \times 10^4 \text{ Pa s}$ at 20°C) and an overriding plate (neutrally buoyant with $\rho = 1428 \text{ kg/m}^3$ and $\eta_{OP} = 6.01 \times 10^4 \text{ Pa s}$ at 20°C). The lower layer is made of a linear-viscous low-viscosity glucose syrup ($\rho = 1428 \text{ kg/m}^3$ and $\eta_{UM} = 289\text{--}291 \text{ Pa s}$), which continues down to 13.3 cm depth (scaling to 665 km of the upper mantle in nature; note that 1 cm scales to 50 km in nature). As such, the rigid bottom of the tank represents the upper-lower mantle discontinuity. The thickness of the subducting plate is 2.0 cm (scaling to 100 km) while that of the overriding plate is 1.5 cm (scaling to 75 km). The width of both plates is 15 cm (scaling to 750 km). The density contrast between the subducting plate and the upper mantle is 100 kg/m^3 . A homogeneous lubricant mixture of petrolatum and paraffin oil (with a weak viscoplastic rheology and $\sim 0.8\text{--}1.5 \text{ Pa}$ flow stress at a shear strain rate of 0.01 s^{-1}) is brushed on the top-surface of the subducting plate to obtain a low mechanical coupling at the subduction zone interface, following the procedure described in Duarte et al. (2013). A 1 mm thick layer of this mixture simulates 5 km of weak hydrated sediments and serpentinized oceanic crust in nature. In our experiment the Reynolds number is very low ($3.2 \times 10^{-6}\text{--}2.1 \times 10^{-5}$, maximally). This ensures that in-

Download English Version:

<https://daneshyari.com/en/article/6427531>

Download Persian Version:

<https://daneshyari.com/article/6427531>

[Daneshyari.com](https://daneshyari.com)